

### **MALAYSIAN JOURNAL OF ANALYTICAL SCIENCES**



Journal homepage: https://mjas.analis.com.my/

## **Research Article**

Enhanced photocatalytic degradation of perfluorooctanoic acid (PFOA) by using MoS<sub>2</sub>/GO/CMC composites: Impact of irradiation conditions, solution pH, and stability for sustainable water treatment

Syafarina Farisa Sateria<sup>1</sup>, Kavirajaa Pandian Sambasevam<sup>2,3</sup>, Ahmad Husaini Mohamed<sup>1</sup>, Zulhatiqah Zolekafeli<sup>1</sup>, and Siti Nor Atika Baharin<sup>1,2\*</sup>

Received: 29 September 2024; Revised: 7 April 2025; Accepted: 9 April 2025; Published: 1 June 2025

#### **Abstract**

This study investigated the removal of perfluorooctanoic acid (PFOA) by using molybdenum disulphide-graphene oxide-carboxymethyl cellulose (MoS<sub>2</sub>/GO/CMC) composites as a photocatalyst under various irradiation conditions and solution pH value levels. The performance of MoS<sub>2</sub>/GO/CMC was compared with MoS<sub>2</sub>/CMC and GO/CMC composites. Under LED light irradiation (12 W, 400–700 nm spectrum range), the MoS<sub>2</sub>/GO/CMC composite achieved a maximum PFOA degradation efficiency of 92.26% within 2 h, outperforming other photocatalysts. The incorporation of cellulose improved nanoparticle stability and increased surface-active sites, enhancing degradation efficiency. pH 5 was found to be optimal for PFOA degradation due to favorable hydrophobic interactions, while higher pH levels hindered degradation due to Coulombic repulsion. Increasing LED wattage to 12 W maximised degradation efficiency by enhancing photodecomposition. These findings provide valuable insights into optimising PFOA degradation under different environmental conditions, highlighting the potential of MoS<sub>2</sub>/GO/CMC composites for sustainable water treatment solutions.

Keywords: carboxymethyl cellulose, perfluorinated compounds, photocatalyst, graphene oxide, hydrogels

### Introduction

Perfluorooctanoic acid (PFOA) belongs to a class of per- and polyfluoroalkyl substances (PFAS), which have been widely used in various industrial and consumer applications due to their exceptional thermal, chemical, and biological stability [1,2,3]. However, these same properties contribute to their persistence in the environment and potential bioaccumulation, raising significant health and ecological concerns [4,5,6]. The strong carbon-fluorine (C-F) bonds make PFOA highly resistant to natural degradation, leading to its widespread detection in water bodies, soil and even human biological [7,8,9]. A study conducted by Mohamad Haron found PFOA concentrations that ranged from 0.31 ng/g to 3693.96 ng/g in household dust from

urban areas, such as Petaling Jaya, Putrajaya and Kuala Lumpur, demonstrated its prevalence in residential environments [10]. Additionally, PFAS, particularly PFOS, have been detected in almost all food categories, with the highest concentrations observed in canned foods (0.18 ng/g – 34.5 ng/g). Alarmingly, hazard quotient (HQ) values exceeding 1 suggest a significant risk to human health [11,12].

The persistent nature of PFOA necessitates the development of effective remediation techniques to mitigate its environmental and health risks. Several methods have been explored for PFOA removal, including adsorption [13], membrane separation [14], microbial degradation [15] and electrochemical degradation [16]. Among these, photocatalysis has

<sup>&</sup>lt;sup>1</sup>School of Chemistry and Environment, Faculty of Applied Sciences, Universiti Teknologi MARA, Cawangan Negeri Sembilan, Kampus Kuala Pilah, 72000 Kuala Pilah, Malaysia

<sup>&</sup>lt;sup>2</sup>Advanced Material for Environmental Remediation (AMER) Research Group, Faculty of Applied Sciences, Universiti Teknologi MARA Cawangan Negeri Sembilan Kampus Kuala Pilah, 72000 Kuala Pilah, Negeri Sembilan, Malaysia

<sup>&</sup>lt;sup>3</sup>Electrochemical Material and Sensor (EMas) Group, Universiti Teknologi MARA, 40450 Shah Alam, Selangor, Malaysia

<sup>\*</sup>Corresponding author: atikabaharin@uitm.edu.my

emerged as a promising and environmentally friendly approach due to its ability to degrade PFOA without secondary pollution [17,18]. In a photocatalytic system, light energy excites the surface electron of photocatalyst, leading to the generation of reactive species that will break down pollutants into less harmful compounds [19].

Amongst various photocatalysts, two-dimensional (2D) semiconductor-based materials have gained attention due to their visible-light activity and high surface-to-volume ratio, enabling efficient charge transfer and light absorption. Transition-metal oxides such as ZnO, TiO2, WO3 as well as sulfides like MoS<sub>2</sub> and CdS, have been explored for their photocatalytic applications [20,21,23]. Molybdenum disulfide (MoS<sub>2</sub>) has attracted particular interest due to its tunable bandgap, strong visible-light absorption, and high adsorption capacity, making it an excellent candidate for organic pollutant degradation [24]. However, to enhance photocatalytic efficiency and reduce electron-hole recombination, MoS<sub>2</sub> is often combined with other materials such as carbon particles [25], titanium oxide nanoparticles [26], and zinc oxide [27]. Amongst these, graphene oxide (GO) has emerged as a highly effective co-catalyst due to its high electrical conductivity, large surface area, and ability to act as an electron acceptor, thereby facilitating charge separation and enhancing photocatalytic activity [28]. In this study, MoS<sub>2</sub> was integrated with GO to improve its overall photocatalytic performance.

To address challenges associated with nanoparticle aggregation and recovery, immobilisation within a hydrogel matrix was explored as a strategy for enhancing photocatalyst stability and reusability. Amongst natural polysaccharides, carboxymethyl cellulose (CMC) stands out due to its water solubility, biocompatibility, and ability to form hydrogels with excellent mechanical stability [29-36]. Unlike other polysaccharides such as chitosan and lignin, CMC offers superior dispersibility, which facilitates uniform photocatalyst distribution and enhances availability of surface-active site. Previous studies had demonstrated the successful integration of cellulose-based hydrogels with various nanomaterials, such as nano chitosan/TiO<sub>2</sub> [37], dot/ZnO [38], Ag/AgCl polyaniline/GO [40], yielding efficient photocatalysts for pollutant degradation. The presence of CMC in MoS<sub>2</sub>/GO composites is expected to further enhance photocatalytic efficiency by stabilising nanoparticles and preventing their agglomeration [41].

Additionally, the choice of light source plays a crucial role in determining photocatalytic efficiency. Light-emitting diodes (LEDs) have gained popularity

as an energy-efficient alternative to conventional UV lamps and mercury-based fluorescent lights due to their longer lifespan, low energy consumption, and tunable spectral output [29]. Unlike traditional sources, LEDs emit a narrow spectrum of visible light, ensuring optimal energy utilisation for photocatalysis while minimising heat loss [30]. Their compact design also allows for flexible reactor configurations, making them suitable for scalable water treatment applications. Despite these advantages, few studies had explored the application of LED-activated photocatalysts for PFOA degradation, highlighting the need for further research in this area.

This study aims to develop and characterise MoS<sub>2</sub>/GO photocatalysts immobilised in a CMC hydrogel matrix for the efficient photodegradation of PFOA under visible-light LED irradiation. The photocatalytic activity of MoS<sub>2</sub>/GO/CMC is evaluated under different reaction conditions, including pH and LED wattage, to determine the optimal degradation parameters. Additionally, the recyclability of the photocatalyst is assessed to demonstrate its potential for sustainable water treatment applications. By integrating an energy-efficient light source with a heterogeneous MoS<sub>2</sub>/GO/CMC hydrogel system, this study seeks to provide an effective and environmentally friendly approach for PFOA remediation.

## Materials and Methods Materials

In this research, sodium molybdate (Na<sub>2</sub>MoO<sub>4</sub>, 98%), sulfuric acid (H<sub>2</sub>SO<sub>4</sub>, 98%), graphite powder (particle size: 20  $\mu$ m), potassium permanganate (KMnO<sub>4</sub>, 99%), sodium carboxymethyl cellulose (MW: ~250,000 g/mol, 99.5%), and perfluorooctanoic acid (PFOA) were obtained from Sigma-Aldrich Co. (St. Louis, Missouri, USA). Thiourea (CH<sub>4</sub>N<sub>2</sub>S,  $\geq$ 99.0%), sodium hydroxide (NaOH), hydrogen peroxide (H<sub>2</sub>O<sub>2</sub>), and sodium nitrate (NaNO<sub>3</sub>) were procured from R&M Chemicals (United Kingdom).

#### Instrument

A Spectrum 100 FTIR Spectrometer from Perkin Elmer, Attenuated Total Reflectance-Fourier Transform Infrared (ATR-FTIR)-FTIR was utilised to examine the functional group in hydrogels with wavenumber ranges of 4000-650 cm<sup>-1</sup>.

# Preparation of MoS2/GO/CMC hydrogels

MoS<sub>2</sub> and GO were prepared according to [18]. The synthesis started with the addition of 0.1 g of MoS<sub>2</sub> and 0.1 g of GO nanoparticles to 2.5 mL of isopropyl alcohol. This mixture was rapidly agitated at 60°C for 1 h. Another solution was created simultaneously by mixing 0.4 g of CMC with 2.5 mL of deionised

water and vigorously swirled. After both solutions were stirred for 1 h, the MoS2 and GO dispersed solution was carefully introduced into the CMC solution while stirring it for 20 min. Then, the resulting gel was processed to form flat beads. The product was finally dried in a desiccator for 48 h [31]. For control samples MoS<sub>2</sub>/CMC and GO/CMC hydrogels were prepared by adding 0.1 g of MoS<sub>2</sub> nanoparticles to 2.5 mL of isopropyl alcohol and agitated vigorously at 60°C for 1 h. Consequently, 0.4 g of CMC was added to 2.5 mL of deionised water and subjected to intense stirring at the same temperature for 1 h. The MoS<sub>2</sub> solution was carefully poured into the CMC solution and stirred for another 20 min. The resulting gel was moulded into flat beads. Finally, the product was dried in a desiccator for 48 h. The preparation of GO/CMC hydrogels followed a similar procedure, with the key difference.

#### Photocatalytic degradation studies

The photodegradation experiments were conducted in a custom-designed photoreactor equipped with an LED light source ( $\lambda = 420-700$  nm, visible light spectrum) with a maximum power of 12 W. The irradiation time for each experiment was set at 180 min to achieve optimal degradation. To evaluate the photocatalytic efficiency of MoS<sub>2</sub>/CMC, GO/CMC, and MoS<sub>2</sub>/GO/CMC in degrading PFOA, a photoreactor (Figure 1) which contained multiple quartz tube reactors was used. In a typical experiment, 0.01 g of the photocatalyst was added to a 10 mL PFOA stock solution (50 mg/L). Before exposure to light, the solutions were stirred in the dark for 30 min to establish an adsorption/desorption equilibrium. Them, the photocatalytic reactions were initiated under LED irradiation (420 nm -700 nm) at varying power levels (7 W, 9 W, 12 W). After treatment, the solutions were filtered and the concentration of PFOA was analysed by using HPLC-UV at 210 nm.

#### Effect of light source

The photocatalytic performance of MoS<sub>2</sub>/CMC, GO/CMC, and MoS<sub>2</sub>/GO/CMC was evaluated under different light sources (dark, UV, fluorescent, and LED). Each composite (0.01 g) was added to 20 mL of 50 mg/L PFOA solution in separate photoreactor tubes. The mixtures were exposed to the respective light sources for degradation, followed by filtration. The PFOA concentration was analysed by using HPLC-UV at 210 nm.

### Effect of pH value

The effect of pH value on PFOA degradation was investigated by using a 50 mg/L PFOA solution across a pH value range of from 2.0 to 12.0. The pH value was adjusted by using HCl or NaOH at 25°C. Then, hydrogels were introduced to the pH-adjusted solution, sonicated for 30 min, and transferred to a glass cuvette for photocatalytic degradation in a UV photoreactor. Afterward, the solutions were filtered, and the PFOA concentration was analysed by using HPLC-UV at 210 nm.

#### Zero potential analysis

The zero point of charge (pHZPC) of MoS<sub>2</sub>/GO/CMC was determined by using the salt addition method. A solution of 0.1 M NaCl (40 mL) was prepared and adjusted to pH 2–10 by using HCl or NaOH. Then, 0.1 g of the material was added, and the suspensions were stirred at 250 rpm overnight. The final pH values were recorded, and the ΔpH (pHf– pHi) was plotted against pHi to determine pHZPC [32-33].



Figure 1. A customised schematic measurement

## Effect of power watt

The photocatalytic performance of MoS<sub>2</sub>/GO/CMC was evaluated under different power watt (7, 9, 12). Each composite (0.01 g) was added to 20 mL of 50 mg/L PFOA solution in separate photoreactor tubes. The mixtures were exposed to the respective light sources for degradation, followed by filtration. The PFOA concentration was analysed by using HPLC-UV at 210 nm.

## Analytical technique

A High-Performance Liquid Chromatography (HPLC) with a UV detector system was used to measure the concentration of PFOA in the aqueous phase. The Agilent 1100 series HPLC system used had a manual sample injector with a degasser, a 20-L injection volume, a column oven that was kept at 40°C, and a pump. A C18 separation column was utilised for the analysis. The samples were eluted at 1.0 mL/min with acetonitrile and aqueous sodium dihydrogen phosphate (5 mMol, pH 7.0) as the mobile phase in a 50:50 (v/v) ratio. of 210 nm was used for detection. Equation (1) was used to calculate the degradation percentage:

Degradation (%)
$$= \frac{(C_0 - C)}{C_0} \times 100$$
(1)

Where, Co is initial PFOA concentration and C is the PFOA concentration at the end of experiment [17].

# **Results and Discussion**

FTIR spectra for CMC, MoS<sub>2</sub>/CMC, GO/CMC, and MoS<sub>2</sub>/GO/CMC are shown in **Figure 2**. The FTIR spectrum of CMC powder revealed absorption peaks which corresponded to the vibrational frequencies of chemical bonds within the CMC structure. The absorption peak at 1600 cm<sup>-1</sup> corresponded to the carboxylate group (COO<sup>-</sup>), while the peak at 1438 cm<sup>-1</sup> was associated with the asymmetric stretching vibration of carboxylate compound (COO<sup>-</sup>Na). Additionally, strong absorption between 950 cm<sup>-1</sup> and 1250 cm<sup>-1</sup> indicated the presence of ether (-C-O-C-) linkages in the CMC compound [34]. The broad band at 3400 cm<sup>-1</sup> corresponded to O-H stretching, while the peak at 1321 cm<sup>-1</sup> was attributed to the symmetric bending of CH<sub>2</sub> groups.

For MoS<sub>2</sub>, the FTIR spectrum displayed peaks between 692 cm<sup>-1</sup> and 1137 cm<sup>-1</sup>, which were characteristic of Mo-S and S-S bond vibrations, confirming the presence of MoS<sub>2</sub>. The broad peak around 3405 cm<sup>-1</sup> corresponded to O-H stretching and bending modes, likely due to residual water or hydroxyl groups adsorbed on the surface [35]. Meanwhile, for GO, the FTIR spectrum exhibited a peak at 3453 cm<sup>-1</sup>, which attributed to O-H

stretching vibrations and indicated the presence of hydroxyl functional groups. Peaks at 1740 cm<sup>-1</sup> and 1589 cm<sup>-1</sup> corresponded to carbonyl (C=O) and C=C stretching vibrations, respectively, confirming the oxidation of graphite. Additionally, the peak at 1137 cm<sup>-1</sup> represented the epoxy (C-O-C) functional group [36-38].

In the FTIR spectrum of the MoS<sub>2</sub>/GO/CMC composite, all the characteristic peaks of CMC, MoS<sub>2</sub>, and GO were present, confirming the successful formation of the composite material [39]. The skeletal vibration peak for the C-O-C bond appeared at 1057 cm<sup>-1</sup>, while a peak at 865 cm<sup>-1</sup> corresponded to Mo-S and S-S linkages, indicating the incorporation of MoS<sub>2</sub> within the composite matrix. The presence of these characteristic functional groups suggested strong interactions between the components, which might enhance the stability and photocatalytic activity MoS<sub>2</sub>/GO/CMC composite [40].

In this study, the photocatalytic process and performance of MoS<sub>2</sub>/CMC, GO/CMC, and MoS<sub>2</sub>/GO/CMC composites in degrading aqueous PFOA solutions were evaluated. **Figure 3** illustrates the C/Co ratio for these composites under different photocatalyst and irradiation conditions, whereby a higher C/Co ratio indicated lower degradation efficiency. The impact of various radiation sources, including dark, UV, fluorescent, and LED irradiation, was examined for over 120 min. Under dark conditions, all photocatalysts displayed insignificant degradation efficiency, primarily due to physical adsorption mechanisms [41].

Meanwhile, under LED light, MoS<sub>2</sub>/GO/CMC exhibited the highest degradation efficiency (0.08) as compared to MoS<sub>2</sub>/CMC (0.28) and GO/CMC (0.29). Notably, fluorescent light showed better degradation performance than UV light for GO/CMC (0.28) and MoS<sub>2</sub>/GO/CMC (0.25). This enhanced performance was attributed to the synergistic effect of MoS2 and GO within the composite matrix. The inclusion of cellulose improved nanoparticle stability, reducing the likelihood of their separation from the polymer matrix and enhancing the ability of composite to effectively separate photogenerated electron pairs. Additionally, GO increased the number of surfaceactive sites, further improving photocatalytic activity. These findings highlighted the promising potential of MoS<sub>2</sub>/GO/CMC composites for effective photocatalytic degradation, particularly under LED

The study also examined the effect of solution pH value on PFOA degradation at pH 5, 7, and 9 (**Figure** 4) [42]. Results indicated that pH 5 was the most

effective condition, yielding a C/Co ratio of 0.08. This optimal pH value facilitated interaction between PFOA and MoS<sub>2</sub>/GO/CMC, primarily due to hydrophobic interactions between graphene oxide and the hydrophobic tail of PFOA [13]. At higher pH levels, PFOA deprotonation resulted in a negatively charged species, leading to electrostatic repulsion with the negatively charged MoS<sub>2</sub>/GO/CMC surface, and thus reducing degradation efficiency.

For MoS<sub>2</sub>/GO/CMC, the study measured the pH value at the point of zero charge (pHpzc), which was determined to be 5.24 (**Figure 5**). This value indicated a nearly neutral surface charge at this pH value. At higher pH value levels, the presence of excess OH<sup>-</sup> ions led to deprotonation of MoS<sub>2</sub>/GO/CMC, resulting in a negatively charged surface which further hindered interaction with the deprotonated PFOA anions [43,44].

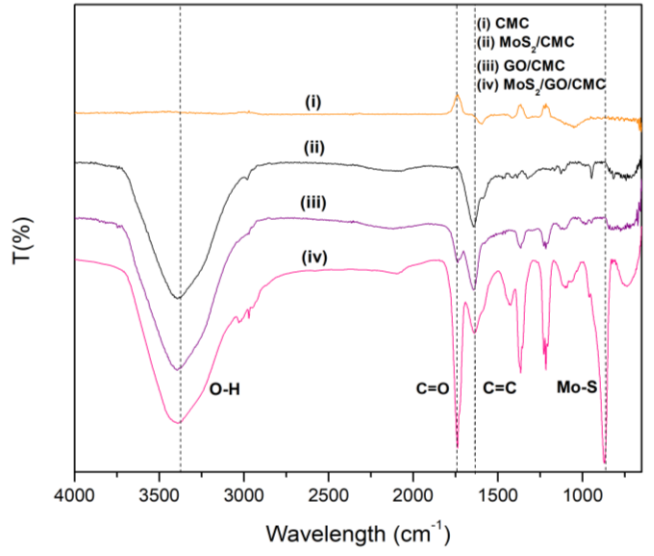


Figure 2. FTIR spectra of (i) CMC, (ii) MoS<sub>2</sub>/CMC, (iii) GO/CMC, and (iv) MoS<sub>2</sub>/GO/CMC composites

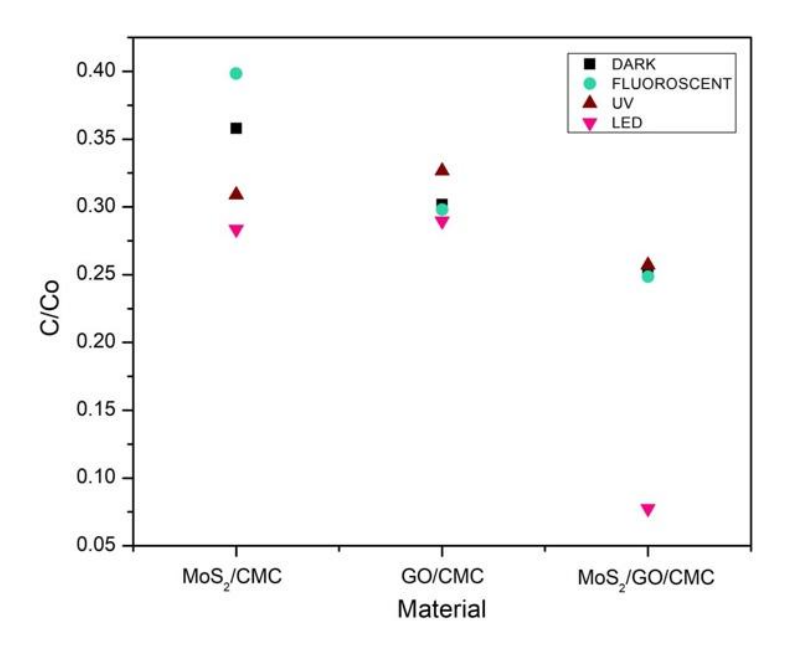
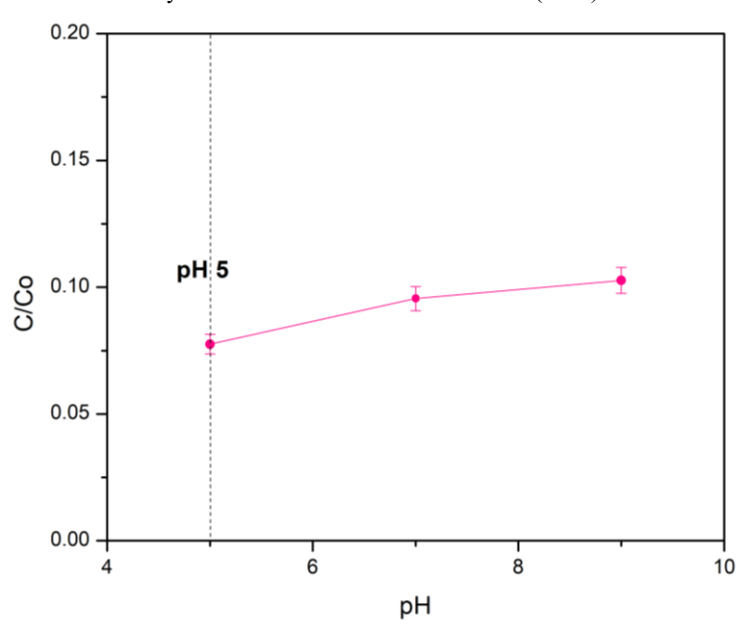


Figure 3. Light sources' influence on PFOA degradation (50 ppm PFOA, pH 2 and 1 g/L of photocatalysts)



**Figure 4.** Influence of pH on PFOA photocatalytic degradation (50 ppm of PFOA, 12 watts of LED light, and 1 g/L of loading catalyst)

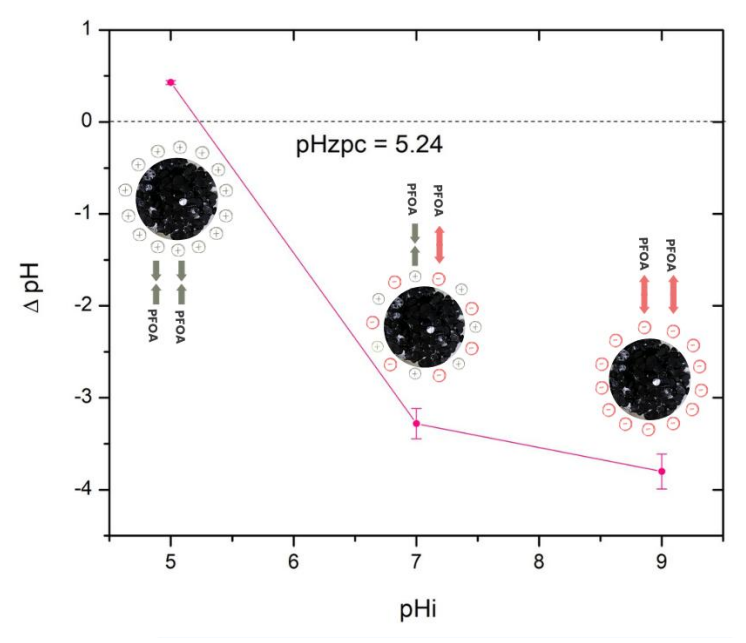


Figure 5. Zero potential (pHpzc) of MoS<sub>2</sub>/GO/CMC (5, 7, 9)

The effect of different wattage levels of emitting diodes (7, 9, and 12 W) on the photocatalytic degradation of PFOA was also investigated. Results showed that 12 watts of power yielded the highest percentage degradation of PFOA (**Figure 6**). This increase in power enhanced the number of quanta

yields available for photodecomposition, thereby improving decomposition efficiency. Overall, these findings offered valuable insights into optimising the photocatalytic degradation of PFOA in various environmental conditions, considering factors such as irradiation, pH value, and power levels [2].

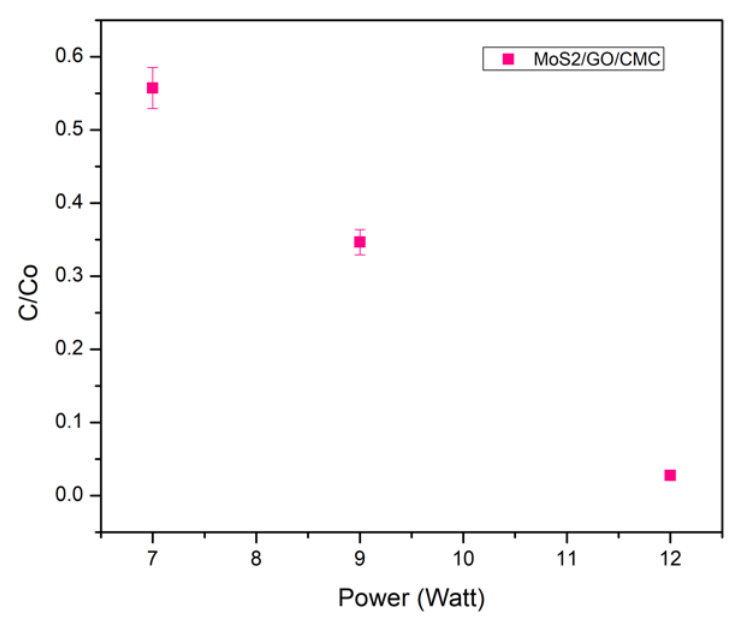


Figure 6. Effect of light source power (watt) of PFOA (1 g/L of loading catalyst, and pH 5) on photocatalytic degradation of PFOA.

The most noteworthy result of photodegradation experiments was a viable photocatalyst that may be renewed. After a few applications, a good photocatalyst ought to be able to maintain good deteriorating performance. The photocatalyst was washed with deionised water and methanol before the experiment, and it was put in oven at 70 °C for 2 h. Figure 7(a) shows that after seven cycles, the deterioration efficiency was decreased by about 12%. Therefore, it was determined that it was allowed to reuse the MoS<sub>2</sub>/GO/CMC for up to seven cycles [45-46]. MoS<sub>2</sub>/GO/CMC structures did not show a significant reduction in efficiency after seven cycles, as seen in Figure 7(a). After seven cycles, the PFOA degradation efficiency decreased from 92.26% to 89.02%, but the deterioration was still significant [47]. Therefore, MoS<sub>2</sub>/GO/CMC revealed high recyclability.

The FTIR analysis of the MoS<sub>2</sub>/GO/CMC composite after the seventh cycle provided insight into the factors which contributed to its reduced photocatalytic degradation efficiency. As shown in **Figure 7(b)**, a noticeable decrease in peak intensity indicated a diminished presence of functional groups

essential for photocatalytic activity. This suggested that repeated use led to the saturation or deactivation of active sites, limiting the functional groups responsible for radical generation. As a result, the ability of composite to generate reactive oxygen species (ROS) declined, reducing its affinity for pollutant molecules and ultimately decreased the degradation rate [48].

Additionally, the absence of the characteristic peak between 1000 cm<sup>-1</sup> and 800 cm<sup>-1</sup> after multiple cycles suggested structural modifications, likely due to the repeated washing of the composite with deionised water [49]. This process may have resulted in the partial removal of functionalised GO components, further reducing available surfaceactive sites. Despite these changes, the composite still maintained a high degradation efficiency after seven cycles, demonstrating its relative stability and reusability. However, the observed decline highlighted the need for potential regeneration strategies or modifications to enhance long-term catalytic performance.

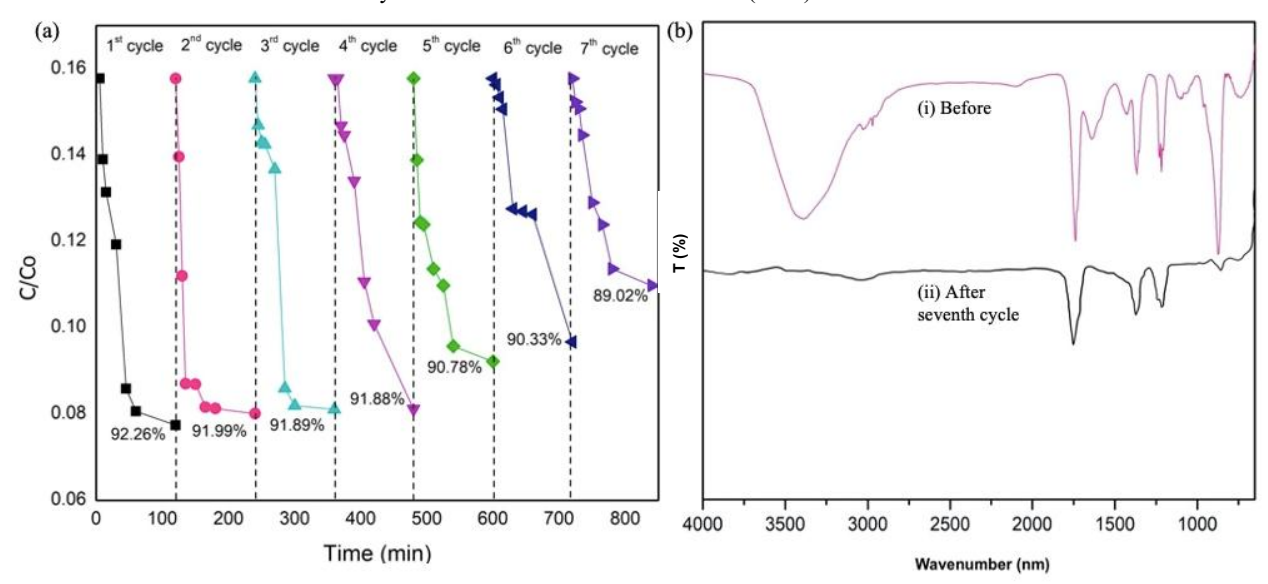


**Figure 7.** (a) The recyclability study of MoS<sub>2</sub>/GO/CMC and (b) FTIR Spectrum of MoS<sub>2</sub>/GO/CMC (i) before and (ii) after the seventh cycle

#### Conclusion

conclusion. this study demonstrates effectiveness of MoS<sub>2</sub>/GO/CMC composites in degrading PFOA under LED light irradiation,  $MoS_2/CMC$ outperforming and GO/CMC composites. The incorporation of cellulose enhanced nanoparticle stability and increased surface-active sites, leading to improved degradation efficiency. The optimal degradation conditions were observed at pH 5, whereby favorable hydrophobic interactions facilitated degradation, whereas higher pH value levels impeded the process. Additionally, increasing the LED wattage to 12W significantly boosted photodecomposition, maximising efficiency. These findings provided valuable insights into optimising PFOA degradation for real-world applications. Future research should explore the long-term stability and reusability of these composites, assess their performance in complex water matrices, and investigate large-scale implementation strategies to advance sustainable water treatment solutions.

## Acknowledgement

We acknowledge the School of Chemistry and Environment, Faculty of Applied Science UiTM Negeri Sembilan, Kuala Pilah Campus for the facilities that have been provided for the research. This project was supported by financial grants such as the Fundamental Research Grant Scheme [FRGS/1/2022/STG05/UITM/02/12] by the Ministry of Higher Education Malaysia.

## References

 Černá, M., Grafnetterová, A. P., Dvořáková, D., Pulkrabová, J., Malý, M., Janoš, T., Vodrážková, N., Tupá, Z., and Puklová, V.

- (2020). Biomonitoring of PFOA, PFOS, and PFNA in human milk from the Czech Republic, time trends, and estimation of infant's daily intake. *Environmental Research*, 188: 109815.
- Li, J., Liu, Y., Song, Y., Cao, L., Dou, Y., Yu, J., Zhang, Y., He, J., Dai, W., Yao, C., and Kong, D. (2024). Enhanced and accelerated degradation of PFOA using visible light—Applying semiconductor carbon nitride as an accelerator. *Journal of Environmental Chemical Engineering*, 12(1): 111653.
- Zhou, J., Yan, J., Qi, X., Wang, M., and Yang, M. (2023). Development of a new matrixcertified reference material for accurate measurement of PFOA and PFOS in oyster meat powder. *Microchemical Journal*, 190: 108746.
- 4. Wee, S. Y., and Aris, A. Z. (2023). Revisiting the "forever chemicals", PFOA and PFOS exposure in drinking water. *NPJ Clean Water*, 6(1): 57.
- Radoor, S., Karayil, J., Jayakumar, A., Kandel, D. R., Kim, J. T., Siengchin, S., and Lee, J. (2024). Recent advances in cellulose- and alginate-based hydrogels for water and wastewater treatment: A review. *Carbohydrate Polymers*, 323: 121339.
- Squadrone, S., Ciccotelli, V., Prearo, M., Favaro, L., Scanzio, T., Foglini, C., and Abete, M. C. (2015). Perfluorooctane sulfonate (PFOS) and perfluorooctanoic acid (PFOA): Emerging contaminants of increasing concern in fish from Lake Varese, Italy. *Environmental Monitoring* and Assessment, 187(7): 4427.
- 7. Suhaimi, N. F., Baharin, S. N. A., Jamion, N. A., Mohd Zain, Z., and Sambasevam, K. P.

- (2023). Polyaniline-chitosan modified on screen-printed carbon electrode for the electrochemical detection of perfluorooctanoic acid. *Microchemical Journal*, 188: 108502.
- 8. Zhang, L., Si, C., Zeng, F., Duan, X., Zhang, D., Xu, W., and Shi, J. (2024). Persulfate activation for efficient remediation of perfluorooctanoic acid (PFOA) and perfluorooctane sulfonic acid (PFOS) in water: Mechanisms, removal efficiency, and future prospects. *Journal of Environmental Chemical Engineering*, 12(1): 111422.
- Vierke, L., Staude, C., Biegel-Engler, A., Drost, W., and Schulte, C. (2012). Perfluorooctanoic acid (PFOA)—Main concerns and regulatory developments in Europe from an environmental point of view. *Environmental Sciences Europe*, 24(1): 16.
- Mohamad Haron, D. E., Yoneda, M., Hod, R., Wahab, M. I. A., and Aziz, M. Y. (2022). Perfluoroalkyl and polyfluoroalkyl substances, bisphenol and paraben compounds in dust collected from residential homes in Klang Valley, Malaysia. *Human Ecological Risk* Assessment, 28(8): 827-843.
- 11. Mohamad Haron, D. E., Yoneda, M., Ahmad, E. D., and Aziz, M. Y. (2023). PFAS, bisphenol, and paraben in Malaysian food and estimated dietary intake. *Food Additives & Contaminants: Part B*, 16(2): 161-175.
- 12. Nguyen, M. D., Sivaram, A. K., Megharaj, M., Webb, L., Adhikari, S., Thomas, M., Surapaneni, A., Moon, E. M., and Milne, N. A. (2023). Investigation on removal of perfluorooctanoic acid (PFOA), perfluorooctane sulfonate (PFOS), perfluorohexane sulfonate (PFHxS) using water treatment sludge and biochar. *Chemosphere*, 338: 139412.
- 13. Hussain, F. A., Janisse, S. E., Heffern, M. C., Kinyua, M., and Velázquez, J. M. (2022). Adsorption of perfluorooctanoic acid from water by pH-modulated Brönsted acid and base sites in mesoporous hafnium oxide ceramics. *IScience*, 25(4): 104138.
- 14. Das, S., and Ronen, A. (2022). A review on removal and destruction of per-and polyfluoroalkyl substances (PFAS) by novel membranes. *Membranes*, 12: 662.
- 15. Karimi Douna, B., and Yousefi, H. (2023). Removal of PFAS by biological methods. *Asian Pacific Journal of Environmental Cancer*, 6(1): 53-68.
- 16. Duinslaeger, N., and Radjenovic, J. (2022). Electrochemical degradation of per- and polyfluoroalkyl substances (PFAS) using low-cost graphene sponge electrodes. *Water Research*, 213: 118148.
- 17. Sateria, S. F., Norsham, I. N., Sambasevam, K.

- P., and Baharin, S. N. A. (2023). Photocatalytic degradation of perfluorooctanoic acid (PFOA) using molybdenum disulphide-graphene oxide composite via Box-Behnken design optimization. *MJChem*, 25(3): 368-377.
- Norsham, I. N. M., Sambasevam, K. P., Shahabuddin, S., Jawad, A. H., and Baharin, S. N. A. (2022). Photocatalytic degradation of perfluorooctanoic acid (PFOA) via MoS2/rGO for water purification using indoor fluorescent irradiation. *Journal of Environmental Chemical Engineering*, 10(5): 108466.
- Pavel, M., Anastasescu, C., State, R.-N., Vasile, A., Papa, F., and Balint, I. (2023). Photocatalytic degradation of organic and inorganic pollutants to harmless end products: Assessment of practical application potential for water and air cleaning. *Catalysts*, 13(2): 380.
- Zheng, X., Wang, H., Wen, J., and Peng, H. (2021). In<sub>2</sub>S<sub>3</sub>-NiS co-decorated MoO<sub>3</sub>@MoS<sub>2</sub> composites for enhancing the solar-light induced CO<sub>2</sub> photoreduction activity. *International Journal of Hydrogen Energy*, 46(74): 36848-36858.
- 21. Jia, F., Yao, Z., and Jiang, Z. (2012). Solvothermal synthesis ZnS-In<sub>2</sub>S<sub>3</sub>-Ag<sub>2</sub>S solid solution coupled with TiO<sub>2</sub>-xSx nanotubes film for photocatalytic hydrogen production. *International Journal of Hydrogen Energy*, 37(4): 3048-3055.
- 22. Ghasemipour, P., Fattahi, M., Rasekh, B., and Yazdian, F. (2020). Developing the ternary ZnO doped MoS<sub>2</sub> nanostructures grafted on CNT and reduced graphene oxide (RGO) for photocatalytic degradation of aniline. *Scientific Reports*, 10(1): 4414.
- 23. Fotiou, D., Lykos, C., and Konstantinou, I. (2024). Photocatalytic removal of the antidepressant fluoxetine from aqueous media using TiO<sub>2</sub> P25 and g-C<sub>3</sub>N<sub>4</sub> catalysts. *Journal of Environmental Chemical Engineering*, 12(1): 111677.
- 24. Liu, J., Du, J., Su, Y., and Zhao, H. (2019). A facile solvothermal synthesis of 3D magnetic MoS<sub>2</sub>/Fe<sub>3</sub>O<sub>4</sub> nanocomposites with enhanced peroxidase-mimicking activity and colorimetric detection of perfluorooctane sulfonate. *Microchemical Journal*, 149: 104019.
- 25. Zhang, J., Wu, J., Yu, J., Zhang, X., He, J., and Zhang, J. (2017). Application of ionic liquids for dissolving cellulose and fabricating cellulose-based materials: *State of the art and future trends. In Materials Chemistry Frontiers*, 1(7): 1273-1290.
- Yan, H., Liu, L., Wang, R., Zhu, W., Ren, X., Luo, L., Zhang, X., Luo, S., Ai, X., and Wang, J. (2020). Binary composite MoS<sub>2</sub>/TiO<sub>2</sub> nanotube arrays as a recyclable and efficient

- photocatalyst for solar water disinfection. *Chemical Engineering Journal*, 401: 126052.
- 27. Ikram, M., Imran, M., Hayat, S., Shahzadi, A., Haider, A., Naz, S., Ul-Hamid, A., Nabgan, W., Fazal, I., and Ali, S. (2022). MoS<sub>2</sub>/cellulose-doped ZnO nanorods for catalytic, antibacterial, and molecular docking studies. *Nanoscale Advances*, 4(1): 211-22.
- Bashir, B., Khalid, M. U., Aadil, M., Zulfiqar, S., Warsi, M. F., Agboola, P. O., and Shakir, I. (2021). CuxNi1-xO nanostructures and their nanocomposites with reduced graphene oxide: Synthesis, characterization, and photocatalytic applications. *Ceramics International*, 47(3): 3603-3613.
- 29. Ghosh, J. P., Langford, C. H., and Achari, G. (2008). Characterization of an LED-based photoreactor to degrade 4-chlorophenol in an aqueous medium using coumarin (C-343) sensitized TiO<sub>2</sub>. *Journal of Physical Chemistry A*, 112(41): 10310-10314.
- 30. Wang, X., and Lim, T. T. (2010). Solvothermal synthesis of C-N codoped TiO<sub>2</sub> and photocatalytic evaluation for bisphenol A degradation using a visible-light irradiated LED photoreactor. *Applied Catalysis B: Environmental*, 100(1–2): 355-364.
- 31. Chen, Y., Cui, J., Liang, Y., Chen, X., and Li, Y. (2021). Synthesis of magnetic carboxymethyl cellulose/graphene oxide nanocomposites for adsorption of copper from aqueous solution. *International Journal of Energy Research*, 45(3): 3988-3998.
- 32. Khan, S. A., Shah, L. A., Shah, M., and Jamil, I. (2021). Engineering 3D polymer network hydrogels for biomedical applications: A review. *Polymer Bulletin*, 79(4): 2685-2705.
- Shah, I., Adnan, R., Wan Ngah, W. S., and Mohamed, N. (2015). Iron impregnated activated carbon as an efficient adsorbent for the removal of methylene blue: Regeneration and kinetics studies. *PLoS ONE*, 10(4): 0122603.
- 34. Hidayat, S., Ardiaksa, P., Riveli, N., and Rahayu, I. (2018). Synthesis and characterization of carboxymethyl cellulose (CMC) from salak-fruit seeds as anode binder for lithium-ion battery. *Journal of Physics: Conference Series*, 1080(1): 012017.
- Lalithambika, K. C., Shanmugapriya, K., and Sriram, S. (2019). Photocatalytic activity of MoS<sub>2</sub> nanoparticles: An experimental and DFT analysis. *Applied Physics A*, 125(12): 817.
- Hosseini, S. A., Mashaykhi, S., and Babaei, S. (2016). Graphene oxide/zinc oxide nanocomposite: A superior adsorbent for removal of methylene blue statistical analysis by response surface methodology (RSM). South

- African Journal of Chemistry, 69: 105-112.
- Bera, M., Chandravati, Gupta, P., and Maji, P. K. (2017). Facile one-pot synthesis of graphene oxide by sonication-assisted mechanochemical approach and its surface chemistry. *Journal of Nanoscience and Nanotechnology*, 18(2): 902-912.
- 38. Bordallo, E., Torneiro, M., and Lazzari, M. (2020). Dissolution of amorphous nifedipine from micelle-forming carboxymethylcellulose derivatives. *Carbohydrate Polymers*, 247: 116699.
- 39. Heidarpour, H., Golizadeh, M., Padervand, M., Karimi, A., Vossoughi, M., and Tavakoli, M. H. (2020). In-situ formation and entrapment of Ag/AgCl photocatalyst inside cross-linked carboxymethyl cellulose beads: A novel photoactive hydrogel for visible-light-induced photocatalysis. *Journal of Photochemistry and Photobiology A: Chemistry*, 398: 112559.
- 40. Zou, L., Qu, R., Gao, H., Guan, X., Qi, X., Liu, C., Zhang, Z., and Lei, X. (2019). MoS<sub>2</sub>/RGO hybrids prepared by a hydrothermal route as a highly efficient catalyst for sonocatalytic degradation of methylene blue. *Results in Physics*, 14: 102458.
- Jubu, P. R., Yam, F. K., Igba, V. M., and Beh, K. P. (2020). Tauc-plot scale and extrapolation effect on bandgap estimation from UV–vis–NIR data A case study of β-Ga<sub>2</sub>O<sub>3</sub>. *Journal of Solid State Chemistry*, 290: 121576.
- 42. Park, K., Ali, I., and Kim, J. O. (2018). Photodegradation of perfluorooctanoic acid by graphene oxide-deposited TiO<sub>2</sub> nanotube arrays in aqueous phase. *Journal of Environmental Management*, 218: 333-339.
- 43. Mancilla, H. B., Cerrón, M. R., Aroni, P. G., Paucar, J. E. P., Tovar, C. T., Jindal, M. K., and Gowrisankar, G. (2022). Effective removal of Cr (VI) ions using low-cost biomass leaves (Sambucus nigra L.) in aqueous solution. Environmental Science and Pollution Research, 2022: 1-14.
- 44. Omorogie, M. O., Babalola, J. O., Unuabonah, E. I., Song, W., and Gong, J. R. (2016). Efficient chromium abstraction from aqueous solution using a low-cost biosorbent: Nauclea diderrichii seed biomass waste. *Journal of Saudi Chemical Society*, 20(1): 49-57.
- 45. Santoso, S. P., Angkawijaya, A. E., Bundjaja, V., Hsieh, C. W., Go, A. W., Yuliana, M., Hsu, H. Y., Tran-Nguyen, P. L., Soetaredjo, F. E., and Ismadji, S. (2021). TiO<sub>2</sub>/guar gum hydrogel composite for adsorption and photodegradation of methylene blue. *International Journal of Biological Macromolecules*, 193(Pt A): 721-733
- 46. Ali, R., Ooi, B. S., (2012). Photodegradation of

- New Methylene Blue N in aqueous solution using zinc oxide and titanium dioxide as catalysts. *Jurnal Teknologi*, 45: 31-42.
- 47. Shi, K., Qian, G., Yi, W., Tang, W., Liu, F., Li, Y., Yang, C., Xiang, Y., and Yao, H. (2024). Magnetic photocatalytic nano-semiconductors prepared from carbon quantum dots compounded with copper ferrate and their application in dye wastewater treatment. *Journal of Environmental Chemical Engineering*, 12(1): 111737.
- 48. Pervaiz, M., Ur Rehman, M., Ali, F., Younas, U., Sillanpaa, M., Kausar, R., Alothman, A. A., Ouladsmane, M., and Mazid, M. A. (2023).

- Biomolecule protective and photocatalytic potential of cellulose supported MoS<sub>2</sub>/GO nanocomposite. *Bioinorganic Chemistry and Applications*, 2023: 3634726.
- Thomas, H. R., Day, S. P., Woodruff, W. E., Vallés, C., Young, R. J., Kinloch, I. A., Morley, G. W., Hanna, J. V., Wilson, N. R., and Rourke, J. P. (2013). Deoxygenation of graphene oxide: Reduction or cleaning? *Chemistry of Materials*, 25(18): 3580-3588.